ACS OMEGA

Article

Cite This: ACS Omega 2018, 3, 15100−15111

http://pubs.acs.org/journal/acsodf

Expanding the Horizon of Multicomponent Oxidative Coupling Reaction via the Design of a Unique, 3D Copper Isophthalate MOF-Based Catalyst Decorated with Mixed Spinel $CoFe_2O_4$ Nanoparticles

Rakesh K. Sharma,* Sneha Yadav, Shivani Sharma, Sriparna Dutta, and Aditi Sharma

Department of Chemistry, Green Chemistry Network Centre, University of Delhi, New Delhi 110007, India

Supporting Information

ABSTRACT: This work discloses the first ever magnetically retrievable copper isophthalate-based metal-organic framework (MOF) decorated with surface-modified cobalt ferrite ($CoFe_2O_4$) nanoparticles that have been utilized as catalytic reactors for obtaining a relatively large number of biologically active benzimidazole scaffolds. A facile one-pot solvothermal approach was employed for obtaining spherical and monodisperse $CoFe_2O_4$ nanoparticles, which were subsequently modified using suitable protecting and functionalizing agents. Finally, these functionalized magnetic nanoparticles were anchored onto the three-dimensional copper isophthalate MOF via a covalent immobilization methodology. The exploitation of advanced microscopic tools such as transmission electron microscopy and scanning electron microscopy provided valuable insights into the morphology of the immobilized MOF. These results indicated that the surface-modified magnetic nanoparticles had grown onto the surface of copper-5-nitroisophthalic acid MOF. A greener C−H functionalization strategy that involves the multicomponent oxidative cross-coupling between two different set of amines (sp^2-hybridized nitrogen-containing anilines and sp^3-hybridized nitrogen-containing alkyl/aryl amine derivatives) and sodium azide has been incorporated to provide access to a broad spectrum of the value-added target benzimidazole moieties. It is interesting to note that this magnetic MOF-catalyzed protocol not only replaces toxic solvents with water, which is a green solvent, but also enhances the economic competitiveness since the magnetic catalyst can be readily recovered and recycled for eight consecutive runs.

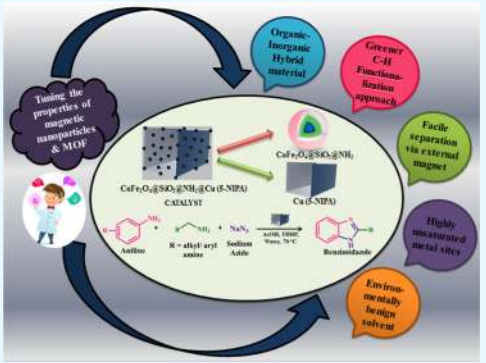

1. INTRODUCTION

Recent years have witnessed a paradigm shift toward green and sustainable organic synthesis. This shift has become even more apparent in the face of growing environmental and economic concerns. It is interesting to note that transition-metal-catalyzed cross-coupling reactions, which lie at the heart of modern innovative science, have experienced a potential economic boom with the advent of C−H activation strategies.[1−13] Introduced by Bergman and co-workers, the C−H activation reactions have gained a paramount importance in the field of synthetic organic chemistry, as they present a major step toward advancing the goals of green chemistry. In this regard, the recent attempts to synthesize C−N bond-containing heterocyclic motifs such as benzimidazoles using an oxidative C−H functionalization strategy are worth applauding.[14−16] Benzimidazole scaffolds are known to show exceptional biological properties that have been exploited successfully in the development of a large number of therapeutic, life-saving drugs such as Nexium, Attacand, Protonix, Prilosec, and Famvir.[17−20] It is the exceptional pharmacological profile of benzimidazole motifs that have stimulated various research groups to explore novel methodologies for the synthesis of these molecules. Among all of the enlisted strategies, C−H activation strategy using multicomponent reaction partners stands apart as it readily overcomes the inherent drawbacks associated with the conventional approaches.[21] However, the utilization of transition-metal salts as catalysts in such cases renders their commercial applicability rather desolate because of the difficulty in separation and recovery of these homogeneous active metal salts. Therefore, the escalation toward the synthesis of an efficient heterogeneous catalyst, which can lead to the generation of desired benzimidazole pharmacophores, is of prime importance.

Currently, metal-organic frameworks (MOFs), an incipient class of porous crystalline materials, have garnered the attention of both academic and industrial researchers for developing heterogeneous catalytic systems.[22−28] The persistent catalytic engrossment of MOFs relies on their exceptional properties, including intrinsic high metal content, well-characterized and tunable crystal structures and composition, multidirectional bonding capability, plentiful metal geometries, and good catalytic selectivity, due to atomically precise active sites that render them appealing for use in catalysis.[29−33] Besides, the coordinatively unsaturated metal sites inside

Received: August 16, 2018
Accepted: October 25, 2018
Published: November 8, 2018

DOI: 10.1021/acsomega.8b02061
ACS Omega 2018, 3, 15100−15111

Scheme 1. Synthesis of 2-Substituted Benzimidazoles via Oxidative Cross-Coupling between Substituted Aniline, Primary Aryl/Alkyl Amine, and Sodium Azide

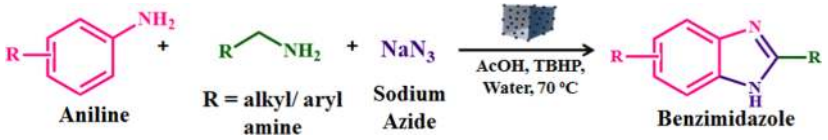

Scheme 2. Schematic Illustration for the Synthesis of $CoFe_2O_4@SiO_2@NH_2@Cu(5\text{-NIPA})$

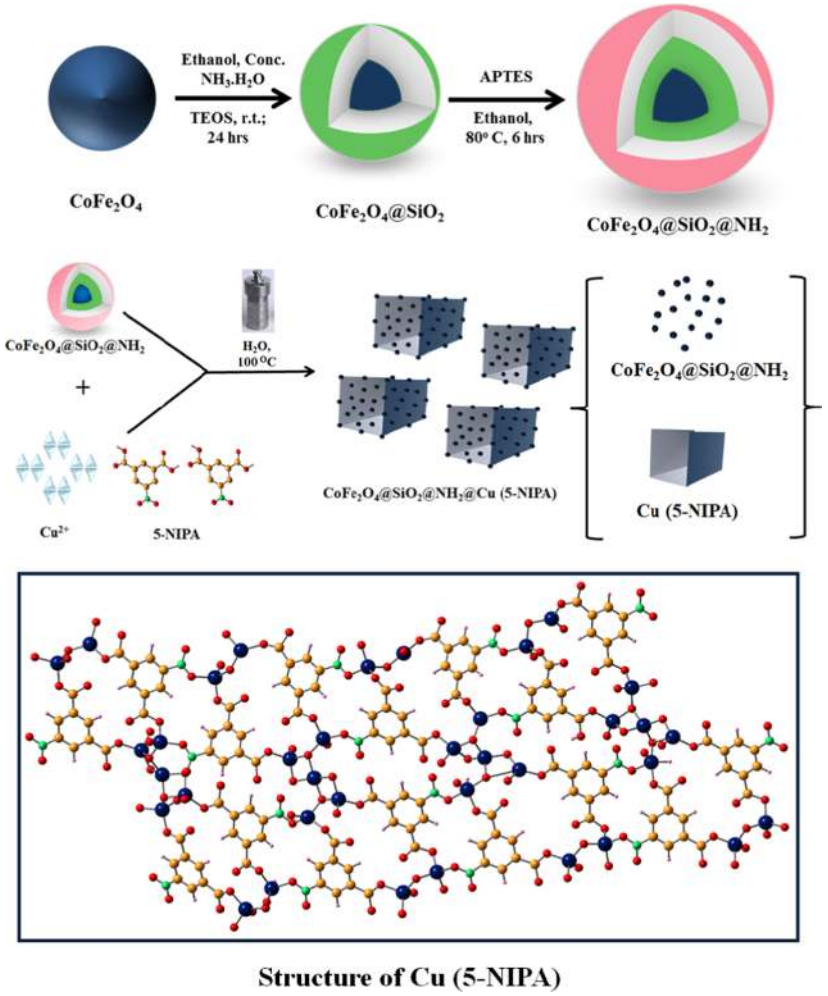

Structure of Cu (5-NIPA)

MOFs possess an inherent ability to tune the interactions between the reactants and the MOF.[34] Perceiving the scientific and industrial impact of these environmentally benign, structurally versatile materials, MOFs having robust backbone structures and high metal-binding sites, in which the structural nodes themselves act as the catalytic centers, have recently been investigated as solid catalysts for catalyzing a wide variety of reactions.[35−37] Also, to enhance the separation properties of the MOFs, the idea of magnetic recoverability has been employed and thus, to date, a few magnetically retrievable MOFs have been reported.[38−45]

1.1. Motivation and Strategy. Considering the quest for developing a sustainable heterogeneous catalyst for the oxidative cross-coupling reaction that can provide a ready access to targeted pharmacological benzimidazoles moieties, and also in conjunction with our ongoing research work in the design and development of magnetic silica-based nanomaterials,[46−53] we report novel $CoFe_2O_4@SiO_2@NH_2@Cu(5\text{-NIPA})$-based MOF as catalyst for the synthesis of exceedingly biologically significant benzimidazoles. Covalent bonding approach is exploited to fabricate MOFs decorated with magnetic nanoparticles (MNPs), which besides enriching the developed material with immense chemical stability, prudent durability, and higher reproducibility, also impart imperishable magnetism.[54−58] This protocol replaces toxic solvents with environmentally benign water, which adds to the green credentials. To the best of our knowledge, this is the first report wherein a heterogeneous catalyst has been effectively employed on multicomponent oxidative coupling for the synthesis of benzimidazoles (Scheme 1).

2. RESULTS AND DISCUSSION

The final catalyst has been prepared by a step-by-step assembly process through the successive surface modifications of cobalt ferrite nanoparticles, as shown in Scheme 2. Preparation of cobalt ferrite nanoparticles is the first step toward the

DOI: 10.1021/acsomega.8b02061
ACS Omega 2018, 3, 15100−15111

accomplishment of the synthesis of catalyst. Cobalt ferrite nanoparticles were synthesized via solvothermal technique.[59] Ethylene glycol plays an important role in the formation of cobalt ferrite nanoparticles. Ethylene glycol, having relatively high boiling point, is a strong reducing agent and has been widely used for the synthesis of monodisperse metal or metal oxide nanoparticles.[60] Magnetic spinel ferrite particles have a strong tendency to undergo agglomeration during their formation in the solution-phase process. Sodium acetate was added for electrostatic stabilization, while poly(ethylene glycol) (PEG) was added as a surfactant. Thereafter, the modified sol−gel approach was utilized for the silica encapsulation of $CoFe_2O_4$ nanoparticles.[61] Subsequently, the amine functionalities were introduced onto the surface of silica-encapsulated cobalt ferrite nanoparticles using 3-aminopropyltriethoxysilane (APTES).[62] Then, a covalent bonding approach was utilized to introduce the synthesized $CoFe_2O_4$@SiO_2@NH_2 onto the copper MOF, which ultimately resulted in the formation of a hybrid magnetic MOF denoted as $CoFe_2O_4$@SiO_2@NH_2@Cu(5-NIPA).

Besides, the structure of developed catalyst was affirmed systematically using different characterization tools such as Fourier transform infrared (FT-IR), X-ray diffraction (XRD), thermogravimetric analysis (TGA), vibrating sample magnetometer (VSM), scanning electron microscopy (SEM), transmission electron microscopy (TEM), energy-dispersive X-ray spectroscopy (EDS), Energy-dispersive X-ray fluorescence (ED-XRF), and inductively coupled plasma mass spectrometry (ICP-MS).

2.1. Catalyst Characterizations. *2.1.1. FT-IR Spectroscopy.* FT-IR spectra of $CoFe_2O_4$, $CoFe_2O_4$@SiO_2, $CoFe_2O_4$@SiO_2@NH_2, and $CoFe_2O_4$@SiO_2@NH_2@Cu(5-NIPA) were recorded in the range of 4000−400 cm^{-1}, as shown in Figure 1.

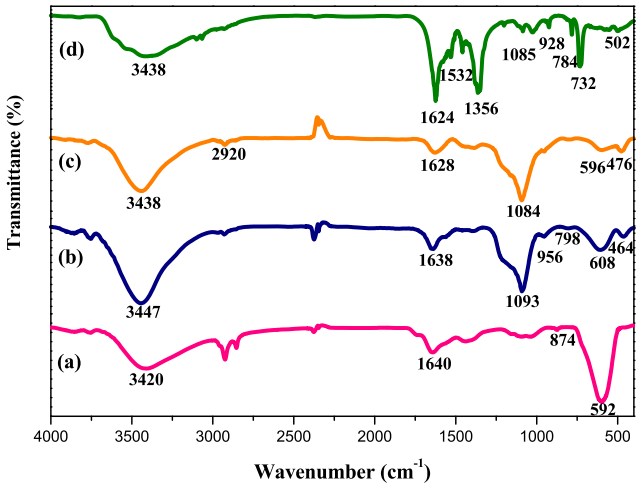

Figure 1. FT-IR spectra of (a) $CoFe_2O_4$, (b) $CoFe_2O_4$@SiO_2, (c) $CoFe_2O_4$@SiO_2@NH_2, and (d) $CoFe_2O_4$@SiO_2@NH_2@Cu(5-NIPA).

The spectrum of $CoFe_2O_4$ clearly depicts absorption bands centered at around 874 and 592 cm^{-1}, which are assigned to the Co−O and Fe−O vibrations, while broad bands at around 3420 and 1640 cm^{-1} are accredited to the stretching and bending vibrations of the surface OH groups. Moreover, appearance of bands at 798, 956, and 1093 cm^{-1} in the spectra of silica-coated cobalt ferrite corresponds to the Si−O−Si symmetric, Si−O symmetric, and Si−O−Si asymmetric stretching modes, which confirms the presence of silica in $CoFe_2O_4$@SiO_2.[63] On moving to APTES-functionalized $CoFe_2O_4$@SiO_2 nanoparticles, two new bands observed at 2920 and 1628 cm^{-1} are attributed to the CH_2 and NH_2 groups of the amino-propyl moiety, respectively, which subsequently confirms the surface functionalization of $CoFe_2O_4$@SiO_2. The comparison of the FT-IR spectra between $CoFe_2O_4$@SiO_2@NH_2 and $CoFe_2O_4$@SiO_2@NH_2@Cu(5-NIPA) confirms that the structure of MOF has been successfully decorated/chemically bonded with amine-functionalized silica-coated cobalt ferrite nanoparticles. In the final spectra of $CoFe_2O_4$@SiO_2@NH_2@Cu(5-NIPA), bands appearing at around 1624, 1356, 1085, 928, and 784 cm^{-1} are assigned to that of the organic ligand (5-nitroisophthalic acid (5-NIPA)). Further, a new weak signal in the spectra of $CoFe_2O_4$@SiO_2@NH_2@Cu(5-NIPA) at 1532 cm^{-1} indicates amide bond formation due to the chemical reaction between the carboxylic groups of (5-NIPA) and exposed NH_2 groups of $CoFe_2O_4$@SiO_2@NH_2.[64−67]

2.1.2. XRD Analysis. The structural integrity of the obtained materials was studied using powder X-ray diffraction (XRD) technique. To deeply understand the crystalline phase structure of $CoFe_2O_4$@SiO_2@NH_2@Cu(5-NIPA), XRD patterns of $CoFe_2O_4$, $CoFe_2O_4$@SiO_2, and $CoFe_2O_4$@SiO_2@NH_2@Cu(5-NIPA) were recorded (Figure 2). The characteristic Bragg diffraction peaks observed at 30.4, 35.7, 43.3, 53.3, 57.3, and 62.9° can be orderly assigned to the (220), (311), (400), (422), (511), and (440) planes of spinel $CoFe_2O_4$. These observation data match well with the standard XRD data of Joint Committee on Powder Diffraction Standards card number (22-1086). Additionally, the Bragg peaks in $CoFe_2O_4$@SiO_2 spectra are obtained at the same 2θ values as $CoFe_2O_4$, which confirms that the structure of cobalt ferrite nanoparticles remains intact even after silica coating. In the XRD spectrum of hybrid magnetic $CoFe_2O_4$@SiO_2@NH_2@Cu(5-NIPA), peaks observed at 2θ values of (8.5), (9.8), (15.75), and (25.98) are assigned to that of crystalline Cu(5-NIPA). Besides, the spectrum also possesses peaks corresponding to spinel cobalt ferrite nanoparticles, which further indicates the decoration of MOF with $CoFe_2O_4$@SiO_2@NH_2.

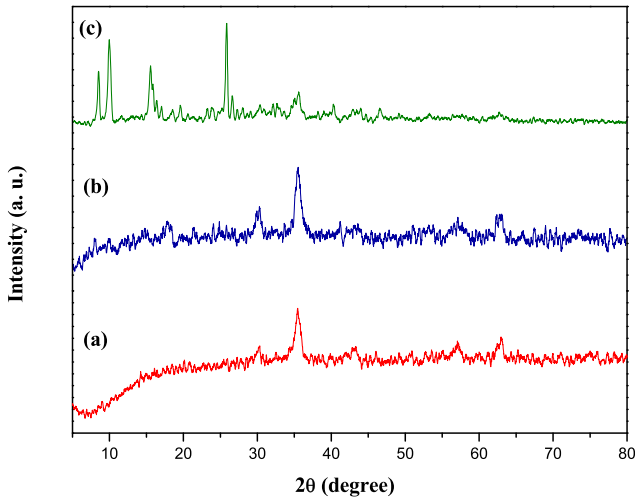

Figure 2. XRD spectrum of (a) $CoFe_2O_4$, (b) $CoFe_2O_4$@SiO_2, and (c) $CoFe_2O_4$@SiO_2@NH_2@Cu(5-NIPA).

DOI: 10.1021/acsomega.8b02061
ACS Omega 2018, 3, 15100−15111

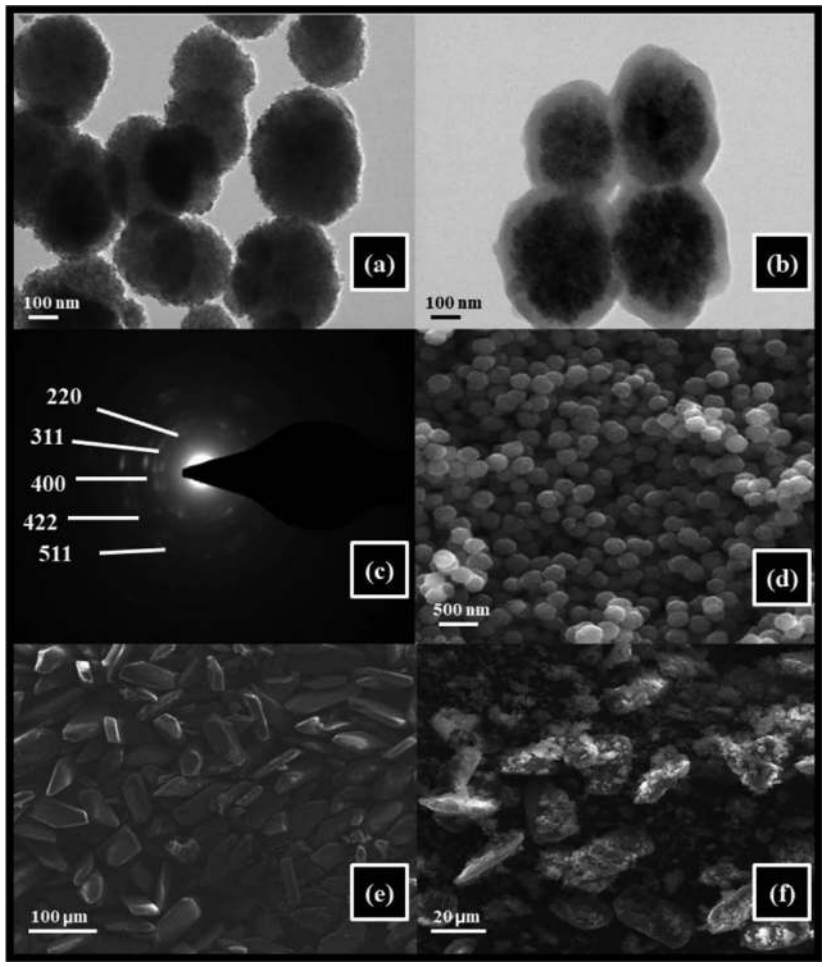

Figure 3. (a) TEM image of synthesized $CoFe_2O_4$ nanoparticles, (b) TEM image of $CoFe_2O_4@SiO_2$, (c) SAED pattern of $CoFe_2O_4$, (d) SEM image of $CoFe_2O_4$, (e) SEM image of Cu(5-NIPA) MOF, and (f) SEM image of hybrid magnetic $CoFe_2O_4@SiO_2@NH_2@$Cu(5-NIPA).

2.1.3. TEM and SEM Analyses. TEM images clearly reveal the monodisperse and spherical structure of $CoFe_2O_4$ nanoparticles with an average diameter of 200 nm (Figure 3). The selected area electron diffraction (SAED) presented the polycrystalline nature of the synthesized nanoparticles and also revealed the appearance of white spotty diffraction rings, which are indexed to [220], [311], [400], [422], and [511] planes of $CoFe_2O_4$. Furthermore, the TEM image of $CoFe_2O_4@SiO_2$ corroborates the presence of a uniform layer of silica of approximately 19 nm around the magnetic core, which further prevents agglomeration. SEM analysis also clearly depicts the monodisperse nature of cobalt ferrite nanoparticles. A close insight into the captured images unveils that the synthesized copper-5-nitroisophthalic acid-based MOF exhibits bipyramidal hexagonal prismlike structure. The SEM images of Cu(5-NIPA) and hybrid magnetic $CoFe_2O_4@SiO_2@NH_2@$Cu(5-NIPA) clearly disclose that the surface of Cu(5-NIPA) has been decorated by amine-functionalized cobalt ferrite nanoparticles.

2.1.4. Physicochemical Characterizations. Energy-dispersive X-ray (EDS) spectroscopy along with elemental mapping and energy-dispersive X-ray fluorescence (ED-XRF) spectroscopy were conducted to accomplish the elemental analysis of the obtained catalyst. EDS elemental mapping images (Figure S1, Supporting Information) of the hybrid magnetic $CoFe_2O_4@SiO_2@NH_2@$Cu(5-NIPA) clearly reveal the uniform distribution of all of the elements, i.e., Fe, Co, Cu, C, N, Si, and O in the MOF. The EDS spectrum of $CoFe_2O_4@SiO_2$ shows well-defined peaks of cobalt, iron, oxygen, and silicon, which substantiates the presence of amorphous silica layer around the magnetic ($CoFe_2O_4$) core (Figure S2). The presence of Cu, N, Co, Fe, O, Si, and C, elements in the spectra of final catalyst further corroborates the decoration of amine-functionalized cobalt ferrite nanoparticles onto MOF. Further, a well-resolved peak of copper in the ED-XRF spectrum of $CoFe_2O_4@SiO_2@NH_2@$Cu(5-NIPA) also supports the covalent anchoring process. Moreover, ICP-MS technique is used to quantify the amount of copper in the obtained catalyst, which was found to be 0.1286 mmol/g.

2.1.5. Thermogravimetric Analysis. TGA was recorded to gain an insight into the stability of the synthesized hybrid magnetic MOF (Figure 4). The thermogram curve of $CoFe_2O_4@SiO_2@NH_2@$Cu(5-NIPA) shows two different regions. A weight loss of around 13% in the first region (i.e., between 40 and 125 °C) is ascribed to the loss of guest and coordinated water molecules from the MOF. Moreover, observation by this analysis elucidates that the complete decomposition of the $CoFe_2O_4@SiO_2@NH_2@$Cu(5-NIPA) structure is observed at 330 °C, i.e., in the second region.

2.1.6. VSM Analysis. The magnetic characteristics of $CoFe_2O_4$, $CoFe_2O_4@SiO_2$, $CoFe_2O_4@SiO_2@NH_2$, and $CoFe_2O_4@SiO_2@NH_2@$Cu(5-NIPA) were investigated using

DOI: 10.1021/acsomega.8b02061
ACS Omega 2018, 3, 15100−15111

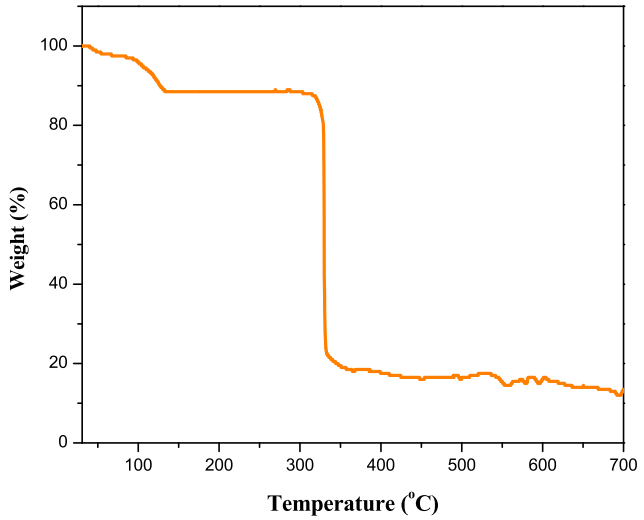

Figure 4. Thermogravimetric analysis (TGA) curve of $CoFe_2O_4$@SiO_2@NH_2@Cu(5-NIPA).

the vibrating sample magnetometer technique (Figure 5). The magnetic hysteresis measurements of the synthesized catalyst

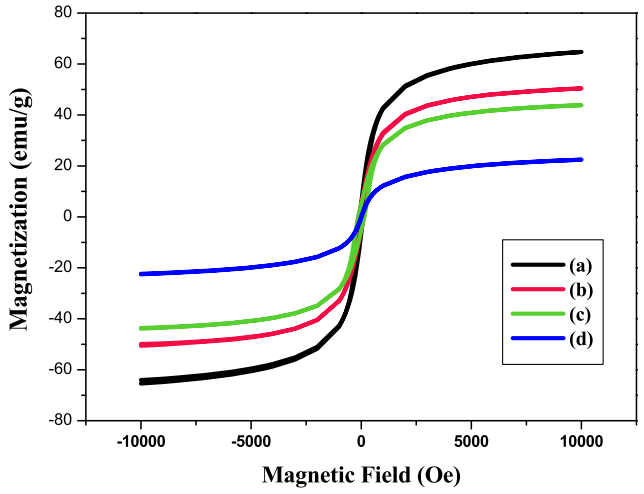

Figure 5. Magnetization curves obtained by VSM at r.t. for (a) $CoFe_2O_4$, (b) $CoFe_2O_4$@SiO_2, (c) $CoFe_2O_4$@SiO_2@NH_2, and (d) $CoFe_2O_4$@SiO_2@NH_2@Cu(5-NIPA).

were carried out at room temperature (r.t.) in external field sweeping between −10 000 and 10 000 Oe. The magnetic hysteresis curves of $CoFe_2O_4$, $CoFe_2O_4$@SiO_2, $CoFe_2O_4$@SiO_2@NH_2, and $CoFe_2O_4$@SiO_2@NH_2@Cu(5-NIPA) reveal the superparamagnetic nature of obtained nanoparticles, which is also signified by the absence of hysteresis phenomenon and coercivity. The specific saturation magnetization (M_s) values of bare $CoFe_2O_4$ nanoparticles, $CoFe_2O_4$@SiO_2, $CoFe_2O_4$@SiO_2@NH_2, final catalyst are found to be 64, 49, 43, and 22 emu/g, respectively. It can be seen that the curve exhibits decrease in the values of saturation magnetization as the surface of bare magnetic nanoparticles is modified using various protecting, functionalizing, and linking agents. This decrease in the net magnetism is observed due to the reduction in the surface moments of individual particles. However, regardless of the lowering of M_s values, it is still considerable and sufficient to collect hybrid MNPs from solution under the influence of external magnetic field.

2.2. Activity of Synthesized Catalyst in the Oxidative Cross-Coupling of Substituted Aniline, 1° Aryl/Alkyl Amine and Sodium Azide To Yield Benzimidazoles via C−H Functionalization Strategy. The catalytic potency of the newly synthesized hybrid core−shell magnetic MOF-based copper catalyst was evaluated in the synthesis of benzimidazoles via C−H functionalization strategy by choosing aniline and benzylamine as model substrates. To achieve the optimum reaction conditions, influence of various kinetic and thermodynamic criterions such as amount of catalyst, solvent, reaction time, temperature, and type of oxidant and its concentration were studied accurately for the oxidative cross-coupling reaction in the presence of $CoFe_2O_4$@SiO_2@NH_2@Cu(5-NIPA) catalyst.

2.3. Catalytic Evaluation. A control experiment using 1:1.2 molar ratios of test substrates (i.e., 1 mmol aniline and 1.2 mmol benzylamine) was first conducted in the absence of catalyst. It was concluded that the reaction failed to occur under such conditions, which necessitates the presence of catalyst to afford the desired benzimidazole product. Various metal-based sources and heterogeneous catalysts were then employed to achieve the target product by cross-coupling between aniline, benzylamine moieties, and sodium azide using *tert*-butyl hydroperoxide (TBHP) as an oxidant (Table S1, Supporting Information). A detailed analysis of the observed results revealed that the newly synthesized copper-MOF-based heterogeneous catalyst resulted in the highest conversion percentage, which further signifies the efficacy of MOF-based copper catalyst in the oxidative cross-coupling reaction.

2.3.1. Amount of Catalyst. Model reactions were carried out to investigate the effect of variation in the amount of catalyst for the cross-coupling reaction using $CoFe_2O_4$@SiO_2@NH_2@Cu(5-NIPA) catalyst and TBHP as an oxidant. The amount of catalyst was varied from 5 to 30 mg. A 44% conversion was observed when 5 mg of $CoFe_2O_4$@SiO_2@NH_2@Cu(5-NIPA) catalyst was employed (Figure 6). A remarkable increase in the conversion percentage was observed

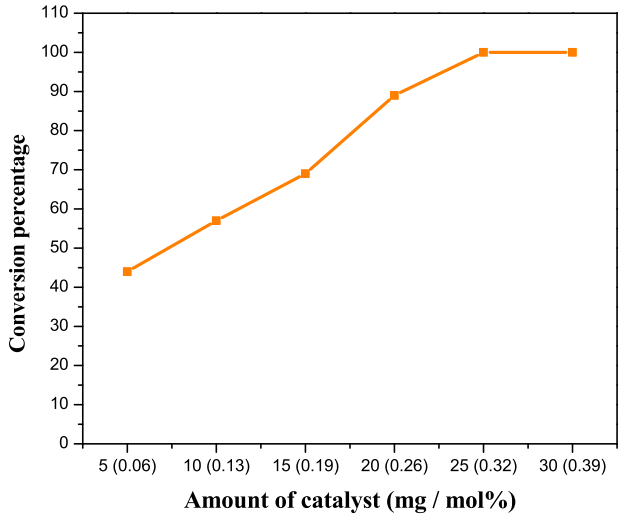

Figure 6. Effect of the amount of catalyst on the oxidative cross-coupling of aniline, benzylamine, and sodium azide [reaction conditions: aniline (1 mmol), benzylamine (1.2 mmol), sodium azide (3 mmol), $CoFe_2O_4$@SiO_2@NH_2@Cu(5-NIPA) catalyst (x mg/y mol %), acetic acid (5 mmol), TBHP (3 mmol) in water (1 mL), 70 °C, 10 h].

DOI: 10.1021/acsomega.8b02061
ACS Omega 2018, 3, 15100−15111

on increasing the amount of catalyst to 25 mg by virtue of increase in the number of active catalytic sites. Further, it was observed that the conversion percentage remained same on increasing the amount of catalyst beyond 25 mg, owing to the exhaustion of all active sites present on the surface of the catalyst. Therefore, the optimized amount of catalyst which resulted in maximum conversion was fixed to be 25 mg or 0.32 mol % for further experiments.

2.3.2. Effect of Various Solvents. Nature of solvent plays a very crucial role in transforming the course of an organic reaction. To achieve the best catalytic conditions, diverse range of solvents such as acetonitrile, ethanol, dimethylformamide, water, dimethyl sulfoxide (DMSO), and toluene were screened for the $CoFe_2O_4$@SiO_2@NH_2@Cu(5-NIPA)-catalyzed cross-coupling reaction (Figure 7). The reaction was also carried out

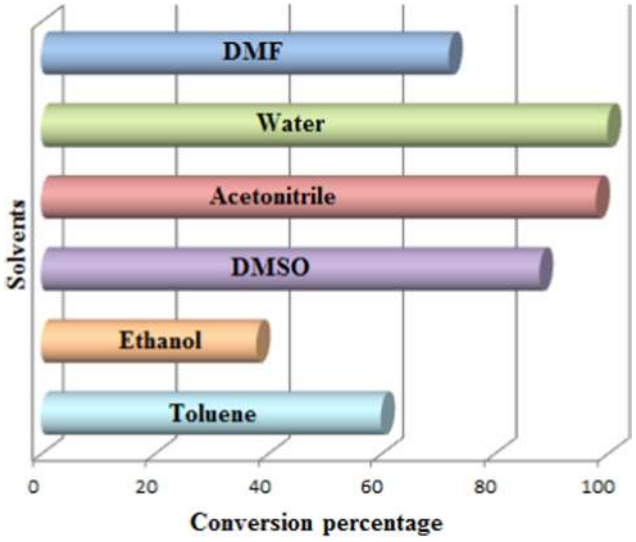

Figure 7. Effect of solvents on the oxidative cross-coupling of aniline, benzylamine, and sodium azide [reaction conditions: aniline (1 mmol), benzylamine (1.2 mmol), sodium azide (3 mmol), $CoFe_2O_4$@SiO_2@NH_2@Cu(5-NIPA) (25 mg/0.32 mol %), acetic acid (5 mmol), TBHP (3 mmol) in solvent (1 mL), 70 °C, 10 h].

under solvent-free conditions, which failed to occur. A self-analysis of the obtained results implies that highest conversion percentage was obtained when water was employed as the solvent. Therefore, further catalytic studies were carried out using water as the solvent.

2.3.3. Effect of Different Oxidants. The oxidizing capabilities of various oxidants such as H_2O_2, TBHP, di-*tert*-butyl peroxide, *tert*-butyl peroxybenzoate (TBPB), and O_2 balloon were explored in the synthesis of benzimidazole motifs via oxidative cross-coupling reaction. The accomplishment of the reaction relies highly on the performance of the employed oxidants. For this purpose, a wide range of oxidants were evaluated in the synthesis of benzimidazoles (Table S2, Supporting Information). The use of oxygen balloon and TBPB resulted in trace amounts of benzimidazoles. It was observed that TBHP was found to be the best oxidizing agent for this particular reaction due to higher conversion percentage.

2.3.4. Effect of Oxidant Concentration. The concentration of TBHP also significantly affects the conversion percentage of product and it was studied by varying its equivalents from 1 to 5 (Figure 8). It was observed that the conversion percentage

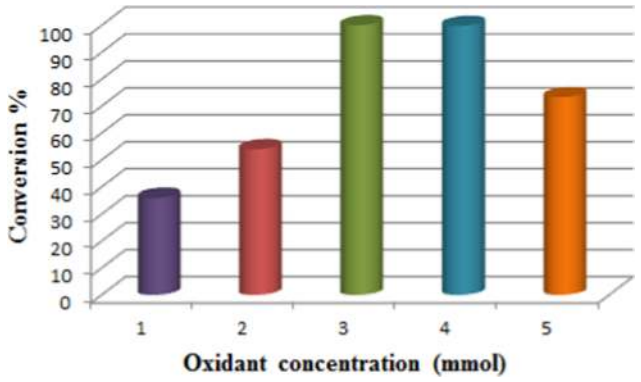

Figure 8. Effect of oxidant concentration on the oxidative cross-coupling of aniline, benzylamine, and sodium azide [reaction conditions: aniline (1 mmol), benzylamine (1.2 mmol), sodium azide (3 mmol), $CoFe_2O_4$@SiO_2@NH_2@Cu(5-NIPA) (25 mg/0.32 mol %), acetic acid (5 mmol), TBHP (*x* mmol) in water (1 mL), 70 °C, 10 h].

increases on increasing the amount of TBHP from 1 to 3 mmol, i.e., from 36 to 100%. Further, an increase in the amount of TBHP led to decrease in conversion percentage because of the enhancement in the side reactions due to large concentration of oxidant. Thus, the amount of oxidant concentration was fixed to 3 equiv for the rest of the experiments.

2.3.5. Effect of Time and Temperature. It was observed that the reaction time and temperature play a pivotal role in enhancing the reaction kinetics. To analyze the effect of these two parameters, model reaction was performed in a distinct range of temperature (40−70 °C) for discrete time periods (Figure 9). Detailed examination of the results displayed that the increase in the reaction temperature leads to linear enhancement in the conversion percentage. Moreover, conversion percentage was found to be increasing on increasing the time from 2 to 10 h. Maximum conversion

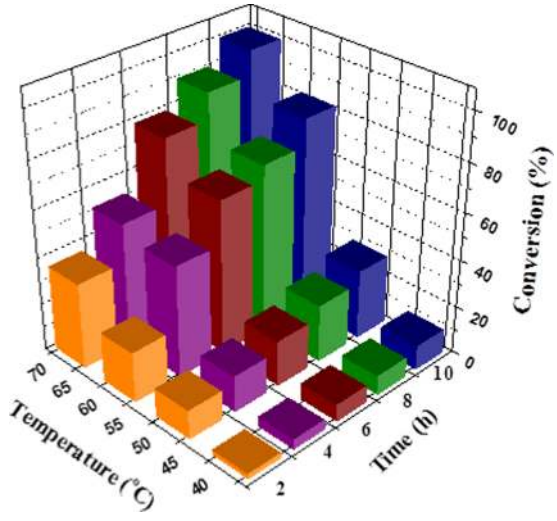

Figure 9. Effects of time and temperature on the oxidative cross-coupling of aniline, benzylamine, and sodium azide [reaction conditions: aniline (1 mmol), benzylamine (1.2 mmol), sodium azide (3 mmol), $CoFe_2O_4$@SiO_2@NH_2@Cu(5-NIPA) catalyst (25 mg/0.32 mol %), acetic acid (5 mmol), TBHP (3 mmol) in water (1 mL)].

DOI: 10.1021/acsomega.8b02061
ACS Omega 2018, 3, 15100−15111

percentage was obtained at 70 °C when the reaction was continued for 10 h. The optimum temperature and time for the coupling reaction were found to be 70 °C and 10 h, respectively.

2.3.6. Substrate Scope. To explore the scope and versatility of this methodology, a series of substituted anilines and primary alkyl/aryl amines were coupled under the established optimal reaction conditions (Table 1). The results indicated that alkyl amines possessing electron-withdrawing and electron-donating groups were efficiently converted into the desired benzimidazole product with high conversion percentage. In general, the protocol exhibited interesting results and the desired benzimidazoles were obtained with high turnover numbers. Further, the protocol was also extended for the heterocyclic substrate such as furfurylamine, which furnished good result. In addition, aliphatic primary amines such as butylamine and 3-phenyl propanamine also underwent reaction. Next, the scope of aniline functionalities was also evaluated for the oxidative coupling protocol. The most distinguishing characteristics of this methodology were high conversion percentage, reaction devoid of unwanted side products, wide substrate applicability, extensive functional group tolerance, and magnetic retrievability.

2.3.7. Mechanistic Pathway. A plausible reaction mechanism has been proposed for the $CoFe_2O_4$@SiO_2@NH_2@Cu(5-NIPA)-catalyzed multicomponent oxidative cross-coupling reaction, as outlined in Scheme 3.[14] The first step involves the oxidation of benzylamine (A) in the presence of TBHP to form imine (B), which further undergoes protonation to form (C). The attack of aryl amine (aniline) on (C) generates complex (D), which then undergoes intramolecular proton exchange to form (E). Loss of ammonia molecule from complex (E) resulted in (F). Complex (F) subsequently undergoes deprotonation to form (G). Copper-based MOF then coordinates with the nitrogen atom of (G)

Table 1. Synthesis of 2-Substituted Benzimidazoles via Oxidative Cross-Coupling between Substituted Aniline, Primary Aryl/Alkyl Amine, and Sodium Azide[a]

Entry	Substituted anilines	1 Aryl/Alkyl amine	Time (h)	[b]Conversion (%)	[c]TON (TOF)
1.	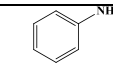	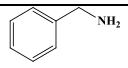	10	100	312 (31)
2.		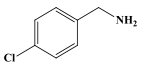	10	100	312 (31)
3.	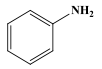	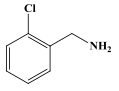	10	91	283 (28)
4.		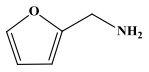	12	93	290 (24)
5.		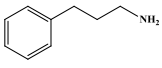	10	31	97 (10)
6.	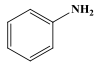	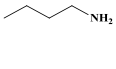	10	17	53 (6)
7.		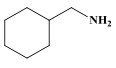	13	54	168 (13)
8.	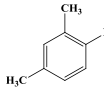	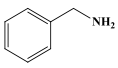	12	39	122 (10)
9.	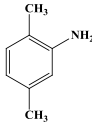	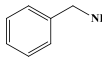	13	57	177 (14)
10.		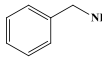	10	6	19 (2)
11.	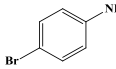	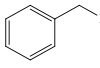	10	5	16 (2)
12.	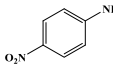	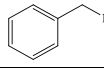	10	–	–

[a]Reaction conditions: substituted aniline (1 mmol), 1° aryl/alkyl amine (1.2 mmol), sodium azide (3 mmol), $CoFe_2O_4$@SiO_2@NH_2@Cu(5-NIPA) (25 mg/0.32 mol %), acetic acid (5 mmol), TBHP (3 mmol) in water (1 mL), 70 °C. [b]Conversion percentages were determined via gas chromatography−mass spectroscopy (GC−MS). [c]TON is the number of moles of the product per mole of the catalyst and TOF = TON per hour.

Scheme 3. Plausible Mechanism for the Oxidative Cross-Coupling Reaction Mediated by $CoFe_2O_4$@SiO_2@NH_2@Cu(5-NIPA)

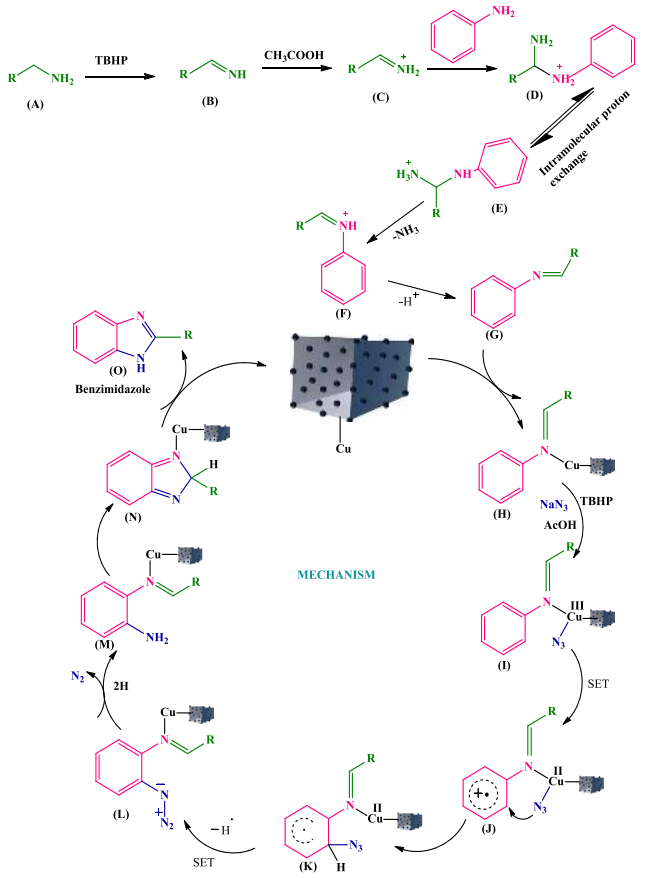

DOI: 10.1021/acsomega.8b02061
ACS Omega 2018, 3, 15100−15111

and forms complex (H). This complex (H) on treatment with sodium azide in the presence of acetic acid (acetic acid is added to generate HN_3 from sodium azide) combines with TBHP to form N_3 radical, which then subsequently coordinates with copper(MOF) to form (I). A single electron transfer (SET) occurs from the aryl ring to the copper metal to generate complex (J), which subsequently transforms into (K) via the transfer of the azido group from copper center to the ortho position of the aryl ring. Complex (K) then undergoes single electron-transfer process to form complex (L), which then generates (M) with the elimination of nitrogen on heating. This complex (M) undergoes intramolecular oxidative cyclization to form (N), which then aromatizes to form the desired product (O), i.e., benzimidazole, while the catalyst is regenerated.

2.4. Heterogeneity Test. Leaching of active metal species from solid support is confronted during catalytic reaction, which is one of the persistent problems in the case of heterogenized homogeneous catalysts. To eliminate the contribution of any homogeneous catalytic species in catalyzed reaction, a standard hot filtration test was performed with model substrates. Although it is a well-known fact that metal-organic frameworks are heterogeneous in nature, just to check the inherent stability of hybrid core−shell magnetic metal-organic framework, catalyst was removed from reaction mixture, when the reaction has been continued for about half the reaction time as found to be 71% by the GC−MS technique. The remaining supernatant components were allowed to react further for about an hour. GC−MS results revealed that the reaction did not proceed further, when the catalyst has been removed, which then debars the possibility of the leaching of active metal species. Further, ICP-MS was also carried out and it was found that there were no traces of copper in the supernatant.

2.5. Recyclability Test. Recyclability and reusability are considered indispensible parameters to assess the feasibility of any heterogeneous catalyst. The recyclability of hybrid magnetic $CoFe_2O_4$@SiO_2@NH_2@Cu(5-NIPA) catalyst in the synthesis of benzimidazole motifs was analyzed under the optimum reaction conditions using aniline and benzylamine as test substrates (Figure 10). Upon completion of the reaction, the catalyst was recovered via an external magnet and washed thoroughly with acetone to remove traces of previous reaction mixture and then dried well under vacuum. The recovered catalyst was then used for successive runs of the same reaction. It was concluded that the catalyst could not only be retrieved successfully but also be used for eight subsequent cycles. The results were further validated by SEM and VSM analyses of the recovered catalyst (Figures S3 and S4, Supporting Information). SEM images showed that no notable change in the size and morphology of recovered catalyst was observed. In addition, the recovered catalyst also exhibited sufficient magnetization value, which allows its facile separation from the reaction mixture via an external magnet. Thus, the synthesized catalyst was found to be stable under applied reaction conditions.

2.6. Comparison of Catalytic Activity of $CoFe_2O_4$@SiO_2@NH_2@Cu(5-NIPA) with the Literature Precedents. A comprehensive literature survey suggests that the as-synthesized catalyst displayed its predominance over previously reported protocols (Table S3, Supporting Information). This is for the first time that a hybrid MOF-based heterogeneous catalyst having high concentration of active catalytic sites has been employed for the synthesis of benzimidazole scaffolds. The presence of a large number of catalytic sites onto the surface of MOF leads to additional binding of substrate molecules. Besides, $CoFe_2O_4$@SiO_2@NH_2@Cu(5-NIPA)-catalyzed protocol is also superior in terms of ambient reaction conditions, high turnover number, extensive functional group tolerance, catalyst recyclability, and magnetic retrievability. Additionally, the present study replaces hazardous solvent DMSO with an environmentally benign solvent, "water". The catalysts that have been reported earlier are homogeneous in nature, which undergoes decomposition immediately after the reaction and thus could not be recovered. On the contrary, the phenomenal structure of MOF hinders catalyst deactivation due to spatial separation of metal centers by organic linkers and thus meticulously overcomes this disadvantage. Moreover, the present catalyst could be magnetically retrieved and recycled for eight successive cycles without any appreciable loss in its catalytic activity. Thus, the present methodology is an attractive alternative for the synthesis of benzimidazole moieties.

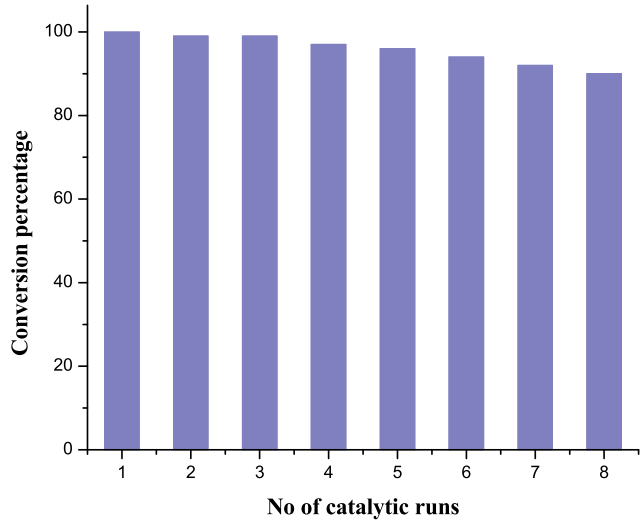

Figure 10. Recycling experiment for the oxidative cross-coupling of aniline, benzylamine, and sodium azide [reaction conditions: aniline (1 mmol), benzylamine (1.2 mmol), sodium azide (3 mmol), $CoFe_2O_4$@SiO_2@NH_2@Cu(5-NIPA) (25 mg/0.32 mol %), acetic acid (5 mmol), TBHP (3 mmol) in water (1 mL), 70 °C, 10 h].

3. CONCLUSIONS

In summary, a novel hybrid magnetic metal-organic framework $CoFe_2O_4$@SiO_2@NH_2@Cu(5-NIPA) having high concentration of reactive metal centers as catalytic sites was fabricated using a chemical bonding approach. The intricately designed $CoFe_2O_4$@SiO_2@NH_2@Cu(5-NIPA)-based hybrid MOF exhibited unrivaled catalytic performance in the synthesis of a broad spectrum of benzimidazoles motifs via oxidative cross-coupling reaction. The modification of $CoFe_2O_4$ nanoparticles with APTES before the assembly process is crucial, as covalent anchoring between $CoFe_2O_4$@SiO_2@NH_2 and Cu(5-NIPA) renders the material with high chemical stability, prudent durability, excellent magnetic response, and good reproducibility without ruining the eccentric structure of MOF. Moreover, it combines the commendatory attributes of both magnetic properties of $CoFe_2O_4$ nanoparticles and remarkable characteristics of MOF. Apart from incomparable catalytic activity, the copper-based MOF catalyst demonstrated broad

DOI: 10.1021/acsomega.8b02061
ACS Omega 2018, 3, 15100−15111

substrate scope, excellent conversion percentage, and high turnover number, and thus a diverse range of benzimidazole scaffolds could be synthesized. The magnetic retrievability of the synthesized catalyst permits its repetitive use in the concerned reaction for consecutive cycles, without any appreciable loss in its catalytic activity and further catalyst also exhibits excellent durability as apparent through heterogeneity test. Besides, the present protocol also employs green reaction conditions (water as the reaction solvent). We anticipated that this novel hybrid MOF-based catalyst that employs water as the reaction solvent will offer a new avenue to economic oxidation catalysts. Moreover, these materials are plausible to be fruitful catalysts for widespread organic transformations and for the synthesis of pharmaceutically pertinent architectures.

4. EXPERIMENTAL SECTION

4.1. Chemicals and Methods. Tetraethyl orthosilicate (TEOS) (99.9%), 3-aminopropyltriethoxysilane (APTES) (98%), and 5-nitroisophthalic acid (5-NIPA) were acquired from Sigma-Aldrich, Fluka, and TCI Chemicals Pvt Ltd., respectively. Copper acetate, ferric chloride, and cobalt chloride were commercially acquired from Sisco Research Laboratory (SRL). All other starting materials and reagents were of analytical grade and obtained from Spectrochem Pvt. Ltd.

4.2. Instrumentation. Fourier transform infrared (FT-IR) spectra were obtained through the KBr pellet method in the range of 4000−400 cm^{-1} using a PerkinElmer Spectrum 2000 FT-IR spectrometer. Powder X-ray diffraction (XRD) was performed using a Bruker, D8 Advance (Karlsruhe, Bundesland, Germany) diffractometer equipped with Cu Kα radiation at a scanning rate of 4°/min in the 2θ range of 5−80° (λ = 0.15405 nm, 40 kV, 40 mA). Transmission electron microscopy (TEM) was conducted using the TECNAI G^2 T30, U-TWIN electron microscope to deduce information regarding the shape and size of the nanoparticles. Besides TEM, scanning electron microscopy (SEM) was carried out to determine the morphology and shape of nanoparticles using a Tescan Mira 3 field emission SEM instrument. First, the samples were prepared by loading on a carbon tape and further coating was done with a thin layer of gold using a sputter coater. Energy-dispersive X-ray spectroscopy (EDS) analysis (equipped with the SEM instrument) was employed for the elemental mapping of the nanocomposites. Energy-dispersive X-ray fluorescence (ED-XRF) spectroscopy was also carried out using a Fischerscope X-ray XAN-FAD BC. A EV-9, Microsense, ADE vibrating sample magnetometer (VSM) was employed for obtaining the magnetization curves of bare and immobilized nanoparticles at r.t. in an applied magnetic field sweeping between −10 000 and 10 000 Oe. The thermal stability of the catalyst was determined using a PerkinElmer Pyris diamond TGA/differential thermal analysis. For obtaining the data, the sample was heated from room temperature to 800 °C in N_2 atmosphere at a heating rate of 10 °C/min and gas flow of 200 mL/min. The inductively coupled plasma mass spectrometry (ICP-MS) analysis was also carried out using ICP-MS (model no.: 7700) to quantify the amount of copper loading onto the catalyst. An Anton Paar Multiwave 3000 microwave instrument equipped with a temperature and pressure sensor was utilized for the microwave-assisted digestion of the catalyst. All of the derived products were analyzed and confirmed through the GC−MS hyphenated technique that was conducted using an Agilent gas chromatograph (6850 GC) with an HP-5MS 5% phenyl methyl siloxane capillary column (30.0 m × 250 μm × 0.25 μm) and a quadrupole mass filter equipped with 5975 mass selective detector using helium as the carrier gas. The isolated yield of 2-substituted benzimidazoles was confirmed by ^{1}H NMR (400 MHz) using a JEOL JNM-AXCP 400.

4.3. Synthesis of Catalyst. *4.3.1. Preparation of Amine-Functionalized Silica-Coated Cobalt Ferrite Nanoparticles.* Magnetic nanoparticles (MNPs) of $CoFe_2O_4$ were synthesized via a facile one-pot solvothermal method that has been reported previously in the literature with slight modifications.[59] First, $CoCl_2{\cdot}6H_2O$ (148.7 mg, 0.625 mmol) and $FeCl_3{\cdot}6H_2O$ (337.9 mg, 1.25 mmol) were dissolved by magnetic stirring at 50 °C in 10 mL of ethylene glycol to form a homogeneous solution. Then, 900 mg of sodium acetate (NaAc) and 500 mg of PEG-6000 were added and the stirring was continued for another 30 min. The above mixed liquor was transferred to a sealed Teflon-lined stainless steel autoclave, which was held at 160 °C for 16 h. The resultant black product was magnetically separated and washed with double-deionized water. Finally, the obtained $CoFe_2O_4$ nanoparticles (0.2 g) were dried at 60 °C for 6 h.

Thereafter, the silica-encapsulated cobalt ferrite microspheres ($CoFe_2O_4$@SiO_2) were prepared by Stöber sol−gel process.[61] In a typical procedure, $CoFe_2O_4$ microspheres (100 mg, 0.426 mmol) were dispersed ultrasonically in a solution containing mixture of 80 mL of ethanol and 20 mL of deionized water. Subsequently, 1.5 mL of ammonia followed by 1 mL of TEOS were added to the mixture solution and the solution was incessantly stirred at room temperature for 24 h. Then, the product was collected by external magnetic forces, washed several times with ethanol and deionized water, and dried under vacuum. Finally, the surface modification of the $CoFe_2O_4$@SiO_2 nanoparticles was accomplished through the introduction of amine groups. For obtaining amine-functionalized silica-coated cobalt ferrite ($CoFe_2O_4$@SiO_2@NH_2) nanoparticles, 2 mL of APTES was added to a well-dispersed solution of 1.0 g of $CoFe_2O_4$@SiO_2 in 200 mL of ethanol.[62] The resulting mixture was stirred continuously at 80 °C for 6 h. The $CoFe_2O_4$@SiO_2@NH_2 nanocomposites were separated via external magnetic field, washed with ethanol several times to remove the unreacted silylating agent, and then finally dried under vacuum.

4.3.2. Preparation of MOFs Decorated with Amine-Functionalized Cobalt Ferrite Nanoparticles. A versatile step-by-step assembly strategy was utilized to fabricate the hybrid magnetic $CoFe_2O_4$@SiO_2@NH_2@Cu(5-NIPA)-based MOF.[35] The as-synthesized amine-functionalized silica-coated cobalt ferrite ($CoFe_2O_4$@SiO_2@NH_2) nanoparticles were dispersed in 10 mL of aqueous solution of $Cu(CH_3COO)_2{\cdot}H_2O$ (0.199 g, 1 mmol) and 5-nitroisophthalic acid (5-NIPA) (0.213 g, 1 mmol). The mixture was first stirred for 15 min to form a gel and then sealed in a Parr reaction vessel and heated at 100 °C for 2 days (Scheme 2). After naturally cooling down to room temperature, very uniform crystalline powder was obtained and further isolated via external magnetic forces. The product was then washed with water and then dried under vacuum to generate the hybrid magnetic $CoFe_2O_4$@SiO_2@NH_2@Cu(5-NIPA) catalyst.

4.4. General Procedure for Hybrid Magnetic $CoFe_2O_4$@SiO_2@NH_2@Cu(5-NIPA)-Catalyzed Synthesis of Benzimidazoles via C−H Functionalization Strategy.

DOI: 10.1021/acsomega.8b02061
ACS Omega 2018, 3, 15100−15111

To a reaction vessel containing a stirred solution of aniline (1.0 mmol), catalyst (25 mg/0.32 mol %), sodium azide (3.0 mmol), acetic acid (5.0 mmol), TBHP (3 mmol) in water (1 mL), and benzylamine (1.2 mmol) were added successively. The resulting reaction mixture was stirred at 70 °C for an appropriate period of time, and the progress of the reaction was monitored via thin-layer chromatography. After completion of reaction, the reaction mixture was cooled to room temperature and the catalyst was separated simply via an external bar magnet. Then, the workup was done by first treating the reaction mixture with saturated $NaHCO_3$ (5 mL) and then extracting using ethyl acetate. The resulting organic layer was separated and then dried over anhydrous sodium sulfate. Finally, the products were analyzed and confirmed using gas chromatography−mass spectroscopy (GC−MS).

4.5. General Procedure for Leaching Experiments. To a reaction vessel, aniline (1.0 mmol), catalyst (25 mg/0.32 mol %), sodium azide (3.0 mmol), acetic acid (5.0 mmol), TBHP (3 mmol) in water (1 mL), and benzylamine (1.2 mmol) were added successively. The resulting reaction mixture was stirred at 70 °C for half the reaction time (i.e., for 5 h). After stirring, the catalyst was removed magnetically and the conversion percentage was determined by GC−MS analysis. The resulting supernatant was further subjected to heating for a prolonged time duration. The GC−MS analysis of the resultant supernatant was carried out once again to check whether any leaching of the active metallic species occurred or not.

4.6. General Procedure for Reusability Experiments. To a reaction vessel, aniline (1.0 mmol), catalyst (25 mg/0.32 mol %), sodium azide (3.0 mmol), acetic acid (5.0 mmol), TBHP (3 mmol) in water (1 mL), and benzylamine (1.2 mmol) were added successively. After completion of the reaction, catalyst was recovered via an external magnet and washed thoroughly with acetone to remove traces of previous reaction mixture and then dried well under vacuum. The recovered catalyst was then used for successive runs of the same reaction.

■ ASSOCIATED CONTENT

Supporting Information

The Supporting Information is available free of charge on the ACS Publications website at DOI: 10.1021/acsomega.8b02061.

Brief statement as noted in text; supporting figures, tables, and spectra (PDF)

■ AUTHOR INFORMATION

Corresponding Author

*E-mail: rksharmagreenchem@hotmail.com. Tel: 011-27666625. Fax: +91-011-2766625.

ORCID

Rakesh K. Sharma: 0000-0003-4281-876X

Author Contributions

The manuscript was written through contributions of all authors. All authors have given approval to the final version of the manuscript.

Notes

The authors declare no competing financial interest.

■ ACKNOWLEDGMENTS

One of the authors, S.Y., expresses her gratitude to the Council of Scientific & Industrial Research (CSIR), New Delhi, India, for the award of a Junior Research fellowship. Also, the authors thank USIC-CLF, DU for FT-IR, TEM, TGA, and VSM analyses.

■ REFERENCES

(1) Yan, R.; Liu, X.; Pan, C.; Zhou, X.; Li, X.; Kang, X.; Huang, G. Aerobic synthesis of substituted quinoline from aldehyde and aniline: Copper-catalyzed intermolecular C−H active and C−C formative cyclization. *Org. Lett.* **2013**, *15*, 4876−4879.

(2) Wei, D.; Zhu, X.; Niu, J. L.; Song, M. P. High-Valent-Cobalt-Catalyzed C−H Functionalization Based on Concerted Metalation Deprotonation and Single-Electron-Transfer Mechanisms. *ChemCatChem* **2016**, *8*, 1242−1263.

(3) Labinger, J. A.; Bercaw, J. E. Understanding and exploiting C−H bond activation. *Nature* **2002**, *417*, 507−514.

(4) Ackermann, L.; Potukuchi, H. K.; Landsberg, D.; Vicente, R. Copper-catalyzed "click" reaction/direct arylation sequence: modular syntheses of 1, 2, 3-triazoles. *Org. Lett.* **2008**, *10*, 3081−3084.

(5) Guo, S.; Qian, B.; Xie, Y.; Xia, C.; Huang, H. Copper-Catalyzed Oxidative Amination of Benzoxazoles via C−H and C−N Bond Activation: A New Strategy for Using Tertiary Amines as Nitrogen Group Sources. *Org. Lett.* **2011**, *13*, 522−525.

(6) Liao, K.; Negretti, S.; Musaev, D. G.; Bacsa, J.; Davies, H. M. Site-selective and stereoselective functionalization of unactivated C−H bonds. *Nature* **2016**, *533*, 230−234.

(7) Davies, H. M.; Manning, J. R. Catalytic C−H functionalization by metal carbenoid and nitrenoid insertion. *Nature* **2008**, *451*, 417.

(8) Simmons, E. M.; Hartwig, J. F. Catalytic functionalization of unactivated primary CH bonds directed by an alcohol. *Nature* **2012**, *483*, 70.

(9) Cuthbertson, J. D.; MacMillan, D. W. The direct arylation of allylic sp^3 C−H bonds via organocatalysis and photoredox catalysis. *Nature* **2015**, *519*, 74.

(10) McNally, A.; Haffemayer, B.; Collins, B. S.; Gaunt, M. J. Palladium-catalysed CH activation of aliphatic amines to give strained nitrogen heterocycles. *Nature* **2014**, *510*, 129.

(11) Zohreh, N.; Jahani, M. NNN-pincer-copper complex immobilized on magnetic nanoparticles as a powerful hybrid catalyst for aerobic oxidative coupling and cycloaddition reactions in water. *J. Mol. Catal. A: Chem.* **2017**, *426*, 117−129.

(12) Pourjavadi, A.; Hosseini, S. H.; Zohreh, N.; Bennett, C. Magnetic nanoparticles entrapped in the cross-linked poly (imidazole/imidazolium) immobilized Cu (II): An effective heterogeneous copper catalyst. *RSC Adv.* **2014**, *4*, 46418−46426.

(13) Zohreh, N.; Hosseini, S. H.; Pourjavadi, A.; Bennett, C. Immobilized copper (II) on nitrogen-rich polymer-entrapped Fe_3O_4 nanoparticles: a highly loaded and magnetically recoverable catalyst for aqueous click chemistry. *Appl. Organomet. Chem.* **2016**, *30*, 73−80.

(14) Mahesh, D.; Sadhu, P.; Punniyamurthy, T. Copper (II)-catalyzed oxidative cross-coupling of anilines, primary alkyl amines, and sodium azide using TBHP: a route to 2-substituted benzimidazoles. *J. Org. Chem.* **2016**, *81*, 3227−3234.

(15) Batra, A.; Singh, P.; Singh, K. N. Cross Dehydrogenative Coupling (CDC) Reactions of N, N-Disubstituted Formamides, Benzaldehydes and Cycloalkanes. *Eur. J. Org. Chem.* **2016**, *2016*, 4927−4947.

(16) Nguyen, K. M. H.; Largeron, M. A Bioinspired Catalytic Aerobic Oxidative C-H Functionalization of Primary Aliphatic Amines: Synthesis of 1, 2-Disubstituted Benzimidazoles. *Chem. Eur. J.* **2015**, *21*, 12606−12610.

(17) Mahesh, D.; Sadhu, P.; Punniyamurthy, T. Copper (I)-catalyzed regioselective amination of N-aryl imines Using $TMSN_3$ and TBHP: A route to substituted benzimidazoles. *J. Org. Chem.* **2015**, *80*, 1644−1650.

DOI: 10.1021/acsomega.8b02061
ACS Omega 2018, 3, 15100−15111

(18) Kim, Y.; Kumar, M. R.; Park, N.; Heo, Y.; Lee, S. Copper-catalyzed, one-pot, three-component synthesis of benzimidazoles by condensation and C−N bond formation. *J. Org. Chem.* **2011**, *76*, 9577−9583.
(19) Kovvuri, J.; Nagaraju, B.; Kamal, A.; Srivastava, A. K. An Efficient Synthesis of 2-Substituted Benzimidazoles via Photocatalytic Condensation of o-Phenylenediamines and Aldehydes. *ACS Comb. Sci.* **2016**, *18*, 644−650.
(20) Bahrami, K.; Khodaei, M. M.; Nejati, A. Synthesis of 1, 2-disubstituted benzimidazoles, 2-substituted benzimidazoles and 2-substituted benzothiazoles in SDS micelles. *Green Chem.* **2010**, *12*, 1237−1241.
(21) Gensch, T.; Hopkinson, M. N.; Glorius, F.; Wencel-Delord, J. Mild metal-catalyzed C−H activation: examples and concepts. *Chem. Soc. Rev.* **2016**, *45*, 2900−2936.
(22) Reinares-Fisac, D.; Aguirre-Díaz, L. M.; Iglesias, M.; Snejko, N.; Gutiérrez-Puebla, E.; Monge, M. A.; Gándara, F. A Mesoporous Indium Metal−Organic Framework: Remarkable Advances in Catalytic Activity for Strecker Reaction of Ketones. *J. Am. Chem. Soc.* **2016**, *138*, 9089−9092.
(23) Chughtai, A. H.; Ahmad, N.; Younus, H. A.; Laypkov, A.; Verpoort, F. Metal−organic frameworks: versatile heterogeneous catalysts for efficient catalytic organic transformations. *Chem. Soc. Rev.* **2015**, *44*, 6804−6849.
(24) Wang, J.-S.; Jin, F.-Z.; Ma, H.-C.; Li, X.-B.; Liu, M.-Y.; Kan, J.-L.; Chen, G.-J.; Dong, Y.-B. Au@Cu(II)-MOF: Highly Efficient Bifunctional Heterogeneous Catalyst for Successive Oxidation−Condensation Reactions. *Inorg. Chem.* **2016**, *55*, 6685−6691.
(25) Serra-Crespo, P.; Ramos-Fernandez, E. V.; Gascon, J.; Kapteijn, F. Synthesis and characterization of an amino functionalized MIL-101 (Al): separation and catalytic properties. *Chem. Mater.* **2011**, *23*, 2565−2572.
(26) Noh, H.; Cui, Y.; Peters, A. W.; Pahls, D. R.; Ortuño, M. A.; Vermeulen, N. A.; Cramer, C. J.; et al. An exceptionally stable metal−organic framework supported molybdenum (VI) oxide catalyst for cyclohexene epoxidation. *J. Am. Chem. Soc.* **2016**, *138*, 14720−14726.
(27) Qin, L.; Hu, J.; Zhang, M.; Li, Y.; Zheng, H. Construction of Metal−Organic Frameworks Based on Two Neutral Tetradentate Ligands. *Cryst. Growth Des.* **2012**, *12*, 4911−4918.
(28) Horiuchi, Y.; Toyao, T.; Saito, M.; Mochizuki, K.; Iwata, M.; Higashimura, H.; Anpo, M.; Matsuoka, M. Visible-light-promoted photocatalytic hydrogen production by using an amino-functionalized Ti (IV) metal−organic framework. *J. Phys. Chem. C* **2012**, *116*, 20848−20853.
(29) Mishra, P.; Edubilli, S.; Mandal, B.; Gumma, S. Adsorption characteristics of metal−organic frameworks containing coordinatively unsaturated metal sites: effect of metal cations and adsorbate properties. *J. Phys. Chem. C* **2014**, *118*, 6847−6855.
(30) Liu, J.; Chen, L.; Cui, H.; Zhang, J.; Zhang, L.; Su, C. Y. Applications of metal−organic frameworks in heterogeneous supramolecular catalysis. *Chem. Soc. Rev.* **2014**, *43*, 6011−6061.
(31) Genna, D. T.; Wong-Foy, A. G.; Matzger, A. J.; Sanford, M. S. Heterogenization of homogeneous catalysts in metal−organic frameworks via cation exchange. *J. Am. Chem. Soc.* **2013**, *135*, 10586−10589.
(32) Wu, P.; Guo, X.; Cheng, L.; He, C.; Wang, J.; Duan, C. Photoactive Metal−Organic Framework and Its Film for Light-Driven Hydrogen Production and Carbon Dioxide Reduction. *Inorg. Chem.* **2016**, *55*, 8153−8159.
(33) Thompson, A. B.; Pahls, D. R.; Bernales, V.; Gallington, L. C.; Malonzo, C. D.; Webber, T.; Tereniak, S. J.; et al. Installing heterobimetallic cobalt−aluminum single sites on a metal organic framework support. *Chem. Mater.* **2016**, *28*, 6753−6762.
(34) Zhao, M.; Yuan, K.; Wang, Y.; Li, G.; Guo, J.; Gu, L.; Hu, W.; Tang, Z.; Zhao, H. Metal−organic frameworks as selectivity regulators for hydrogenation reactions. *Nature* **2016**, *539*, 76−80.
(35) Zhao, Y.; Padmanabhan, M.; Gong, Q.; Tsumori, N.; Xu, Q.; Li, J. CO catalytic oxidation by a metal organic framework containing high density of reactive copper sites. *Chem. Commun.* **2011**, *47*, 6377−6379.
(36) Cirujano, F. G.; Leyva-Pérez, A.; Corma, A.; Llabrés i Xamena, F. X. MOFs as Multifunctional Catalysts: Synthesis of Secondary Arylamines, Quinolines, Pyrroles, and Arylpyrrolidines over Bifunctional MIL-101. *ChemCatChem* **2013**, *5*, 538−549.
(37) Mason, J. A.; Darago, L. E.; Lukens, W. W., Jr.; Long, J. R. Synthesis and O_2 Reactivity of a Titanium (III) Metal−Organic Framework. *Inorg. Chem.* **2015**, *54*, 10096−10104.
(38) Miao, Z.; Shu, X.; Ramella, D. Synthesis of a Fe_3O_4@P4VP@ metal−organic framework core−shell structure and studies of its aerobic oxidation reactivity. *RSC Adv.* **2017**, *7*, 2773−2779.
(39) Zhang, H. Y.; Hao, X. P.; Mo, L. P.; Liu, S. S.; Zhang, W. B.; Zhang, Z. H. Magnetic metal-organic framework as a highly active heterogeneous catalyst for one-pot synthesis of 2-substituted alkyl and aryl (indolyl) kojic acid derivatives. *New J. Chem.* **2017**, *41*, 7108−7115.
(40) Li, J.; Gao, H.; Tan, L.; Luan, Y.; Yang, M. Superparamagnetic Core−Shell Metal−Organic Framework $Fe_3O_4/Cu_3(btc)_2$ Microspheres and Their Catalytic Activity in the Aerobic Oxidation of Alcohols and Olefins. *Eur. J. Inorg. Chem.* **2016**, *2016*, 4906−4912.
(41) Jiang, S.; Yan, J.; Habimana, F.; Ji, S. Preparation of magnetically recyclable MIL-53 (Al)@SiO_2@Fe_3O_4 catalysts and their catalytic performance for Friedel−Crafts acylation reaction. *Catal. Today* **2016**, *264*, 83−90.
(42) Ricco, R.; Malfatti, L.; Takahashi, M.; Hill, A. J.; Falcaro, P. Applications of magnetic metal−organic framework composites. *J. Mater. Chem. A* **2013**, *1*, 13033−13045.
(43) Chen, Y.; Xiong, Z.; Peng, L.; Gan, Y.; Zhao, Y.; Shen, J.; Qian, J.; Zhang, L.; Zhang, W. Facile preparation of core−shell magnetic metal−organic framework nanoparticles for the selective capture of phosphopeptides. *ACS Appl. Mater. Interfaces* **2015**, *7*, 16338−16347.
(44) Li, Y.; Xie, Q.; Hu, Q.; Li, C.; Huang, Z.; Yang, X.; Guo, H. Surface modification of hollow magnetic Fe_3O_4@NH_2-MIL-101 (Fe) derived from metal-organic frameworks for enhanced selective removal of phosphates from aqueous solution. *Sci. Rep.* **2016**, *6*, No. 30651.
(45) Zhao, X.; Liu, S.; Tang, Z.; Niu, H.; Cai, Y.; Meng, W.; Wu, F.; Giesy, J. P. Synthesis of magnetic metal-organic framework (MOF) for efficient removal of organic dyes from water. *Sci. Rep.* **2015**, *5*, No. 11849.
(46) Sharma, R. K.; Dutta, S.; Sharma, S. Quinoline-2-carboimine copper complex immobilized on amine functionalized silica coated magnetite nanoparticles: a novel and magnetically retrievable catalyst for the synthesis of carbamates via C−H activation of formamides. *Dalton Trans.* **2015**, *44*, 1303−1316.
(47) Sharma, R. K.; Sharma, S.; Dutta, S.; Zboril, R.; Gawande, M. B. Silica-nanosphere-based organic−inorganic hybrid nanomaterials: synthesis, functionalization and applications in catalysis. *Green Chem.* **2015**, *17*, 3207−3230.
(48) Sharma, R. K.; Yadav, M.; Monga, Y.; Gaur, R.; Adholeya, A.; Zboril, R.; Gawande, M. B.; et al. Silica-based Magnetic Manganese Nanocatalyst−Applications in the Oxidation of Organic Halides and Alcohols. *ACS Sustainable Chem. Eng.* **2016**, *4*, 1123−1130.
(49) Sharma, R. K.; Dutta, S.; Sharma, S. Quinoline-2-carboimine copper complex immobilized on amine functionalized silica coated magnetite nanoparticles: a novel and magnetically retrievable catalyst for the synthesis of carbamates via C−H activation of formamides. *Dalton Trans.* **2015**, *44*, 1303−1316.
(50) Sharma, R. K.; Dutta, S.; Sharma, S. Nickel (ii) complex covalently anchored on core shell structured SiO_2@Fe_3O_4 nanoparticles: a robust and magnetically retrievable catalyst for direct one-pot reductive amination of ketones. *New J. Chem.* **2016**, *40*, 2089−2101.
(51) Sharma, R. K.; Gaur, R.; Yadav, M.; Rathi, A. K.; Pechousek, J.; Petr, M.; Gawande, M. B.; et al. Maghemite-Copper Nanocomposites: Applications for Ligand-Free Cross-Coupling (C−O, C−S, and C−N) Reactions. *ChemCatChem* **2015**, *7*, 3495−3502.

DOI: 10.1021/acsomega.8b02061
ACS Omega 2018, 3, 15100−15111

(52) Sharma, R. K.; Yadav, M.; Gaur, R.; Monga, Y.; Adholeya, A. Magnetically retrievable silica-based nickel nanocatalyst for Suzuki–Miyaura cross-coupling reaction. *Catal. Sci. Technol.* **2015**, *5*, 2728–2740.
(53) Sharma, R. K.; Monga, Y.; Puri, A.; Gaba, G. Magnetite (Fe_3O_4) silica based organic–inorganic hybrid copper (ii) nano-catalyst: a platform for aerobic N-alkylation of amines. *Green Chem.* **2013**, *15*, 2800–2809.
(54) Hu, Y.; Huang, Z.; Liao, J.; Li, G. Chemical bonding approach for fabrication of hybrid magnetic metal–organic framework-5: high efficient adsorbents for magnetic enrichment of trace analytes. *Anal. Chem.* **2013**, *85*, 6885–6893.
(55) Xu, Y.; Jin, J.; Li, X.; Han, Y.; Meng, H.; Wang, T.; Zhang, X. Fabrication of hybrid magnetic HKUST-1 and its highly efficient adsorption performance for Congo red dye. *RSC Adv.* **2015**, *5*, 19199–19202.
(56) Huang, A.; Dou, W.; Caro, J. Steam-stable zeolitic imidazolate framework ZIF-90 membrane with hydrogen selectivity through covalent functionalization. *J. Am. Chem. Soc.* **2010**, *132*, 15562–15564.
(57) Bristow, J. K.; Butler, K. T.; Svane, K. L.; Gale, J. D.; Walsh, A. Chemical bonding at the metal–organic framework/metal oxide interface: simulated epitaxial growth of MOF-5 on rutile TiO_2. *J. Mater. Chem. A* **2017**, *5*, 6226–6232.
(58) Huang, A.; Bux, H.; Steinbach, F.; Caro, J. Molecular-sieve membrane with hydrogen permselectivity: ZIF-22 in LTA topology prepared with 3-aminopropyltriethoxysilane as covalent linker. *Angew. Chem., Int. Ed.* **2010**, *122*, 5078–5081.
(59) Yang, J.-C.; Yin, X.-B. $CoFe_2O_4$@MIL-100 (Fe) hybrid magnetic nanoparticles exhibit fast and selective adsorption of arsenic with high adsorption capacity. *Sci. Rep.* **2017**, *7*, No. 40955.
(60) Deng, H.; Li, X.; Peng, Q.; Wang, X.; Chen, J.; Li, Y. Monodisperse magnetic single-crystal ferrite microspheres. *Angew. Chem., Int. Ed.* **2005**, *117*, 2842–2845.
(61) Wang, H.; Huang, J.; Ding, L.; Li, D.; Han, Y. A facile synthesis of monodisperse $CoFe_2O_4/SiO_2$ nanoparticles. *Appl. Surf. Sci.* **2011**, *257*, 7107–7112.
(62) Paul, S.; Clark, J. H. Structure-activity relationship between some novel silica supported palladium catalysts: a study of the Suzuki reaction. *J. Mol. Catal. A: Chem.* **2004**, *215*, 107–111.
(63) Ren, C.; Ding, X.; Fu, H.; Li, W.; Wu, H.; Yang, H. Core–shell superparamagnetic monodisperse nanospheres based on amino-functionalized $CoFe_2O_4$@SiO_2 for removal of heavy metals from aqueous solutions. *RSC Adv.* **2017**, *7*, 6911–6921.
(64) Fu, L.; Sá Ferreira, R. A.; Silva, N. J. O.; Carlos, L. D.; de Zea Bermudez, V.; Rocha, J. Photoluminescence and quantum yields of urea and urethane cross-linked nanohybrids derived from carboxylic acid solvolysis. *Chem. Mater.* **2004**, *16*, 1507–1516.
(65) Villanneau, R.; Marzouk, A.; Wang, Y.; Djamaa, A. B.; Laugel, G.; Proust, A.; Launay, F. Covalent grafting of organic–inorganic polyoxometalates hybrids onto mesoporous SBA-15: a key step for new anchored homogeneous catalysts. *Inorg. Chem.* **2013**, *52*, 2958–2965.
(66) Patra, S.; Crespo, T. H.; Permyakova, A.; Sicard, C.; Serre, C.; Chaussé, A.; Steunou, N.; Legrand, L. Design of metal organic framework–enzyme based bioelectrodes as a novel and highly sensitive biosensing platform. *J. Mater. Chem. B* **2015**, *3*, 8983–8992.
(67) Wang, W. J.; Hai, X.; Mao, Q. X.; Chen, M. L.; Wang, J. H. Polyhedral oligomeric silsesquioxane functionalized carbon dots for cell imaging. *ACS Appl. Mater. Interfaces* **2015**, *7*, 16609–16616.

DOI: 10.1021/acsomega.8b02061
ACS Omega 2018, 3, 15100–15111